 doi:10.20944/preprints201807.0346.v1

Research Article

Characterization of mitochondrial GSH transporters and their role in RPE protection

Wang M [1,2], Lau L [2,3], Sreekumar PG[2], Spee C[4], Liu L [1], Hinton DR[4], Sadda SR[2], Kannan R[2]*

[1] Department of Ophthalmology, Renji Hospital, School of Medicine, Shanghai Jiaotong University, Shanghai, China mowang@mednet.ucla.edu; liulin1962rj@126.com
[2] Arnold and Mabel Beckman Macular Research Center, Doheny Eye Institute, Los Angeles, CA 90033, USA. sparameswaran@doheny.org; leliew61@gmail.com; sparameswaran@doheny.org; ssadda@doheny.org; rkannan@doheny.org
[3] Institute of Clinical Medicine, School of Medicine, National Yang-Ming University, Taipei, Taiwan leliew61@gmail.com
[4] Department of Pathology and Ophthalmology, USC Roski Institute, Keck School of Medicine of the University of Southern California, Los Angeles, CA, USA ChristineK.Spee@med.usc.edu; dhinton@usc.edu
* Correspondence: rkannan@doheny.org ; Tel.: +1-323-342-6691

Abstract: Mitochondrial dysfunction and oxidative stress are thought to be relevant to the pathogenesis of age-related macular degeneration (AMD). Glutathione (GSH) homeostasis fulfills a number of important roles in mitochondria, such as maintenance of mitochondrial DNA and respiratory competency of cells. Although the transport of mitochondrial GSH (mGSH) is not fully understood, increasing evidence from non-ocular tissues suggests that OGC (2-oxoglutarate carrier, SLC25A11) and DIC (dicarboxylate carrier, SLC25A10) are involved in mGSH transport. However, whether OGC and DIC mediate the transfer of GSH into the mitochondria of retinal pigment epithelial cells (RPE) remains unknown. Thus, we investigated the expression, localization, and function of OGC and DIC in human RPE (hRPE) in relation to oxidative stress and GSH. Both OGC and DIC are expressed in hRPE and are localized in mitochondria. We also found a dose and time-dependent decrease of OGC and DIC expression under oxidative stress and increased expression in polarized RPE. Our data show that the downregulation of OGC and DIC resulted in increased apoptosis and mGSH depletion which can be overcome by co-treatment with GSH-MEE. These findings suggest that overexpression of OGC and DIC may be an effective strategy to decrease susceptibility to mitochondrial toxicants by elevation of mGSH.

Keywords: Retinal pigment epithelium (RPE) 1; oxidative stress 2; mitochondria 3; apoptosis 4; 2-oxoglutarate carrier (OGC) 5; dicarboxylate carrier (DIC) 6; glutathione (GSH) 7; mitochondrial GSH (mGSH) 8

1. Introduction

Age-related macular degeneration (AMD), a progressive degenerative retinal disease, is the leading cause of irreversible blindness in the elderly and is characterized by the decrease in macular function due to the degeneration of retinal pigment epithelium (RPE) cells [1]. Multiple cellular mechanisms are involved in the dysfunction and death of RPE cells in AMD, including accumulation of toxic metabolites, endoplasmic reticulum (ER) stress , oxidative stress and inflammation [2,3]. The mitochondrial dysfunction and oxidative stress are believed to be the central mechanisms in various pathological conditions, that have been extensively studied in the progression of AMD.

Mitochondria are the powerhouse of mammalian cells and the main generators of reactive oxygen species (ROS), the overgeneration of which leads to oxidative stress. This phenomenon contributes to mitochondrial damage linked to a number of pathological disorders. In addition, they

 doi:10.20944/preprints201807.0346.v1

are considered to play a vital role in controlling the fate of cells through regulation of death pathways [4,5].

Glutathione (GSH), an endogenous antioxidant abundantly present in retina and in retinal pigment epithelial (RPE) cells, is important for the maintenance of cellular viability [6,7]. Intracellular GSH levels are maintained by redox cycling, de novo synthesis, and transmembrane transport, and GSH mainly exists in a thiol-reduced state (GSH) or in an oxidized state (GSSG). Even though GSH is synthesized in the cytosol, it is distributed in intracellular organelles such as mitochondria, nucleus, endoplasmic reticulum (ER) and Golgi complex [8]. However, the glutathione in mitochondrial GSH (mGSH) is mainly found in reduced form and represents a minor fraction of the total cellular GSH pool (10–15%). It works as a critical antioxidant reserve that is derived entirely from the larger cytosolic pool by the action of carrier transporters [9]. Since mGSH plays a significant role in cellular defense against pro-oxidants, the depletion of mGSH affects cell viability, either by predisposing cells to apoptosis or by modulating mitochondrial membrane potential and subsequent activation of caspases, through regulation of redox pathways [10].

Our laboratory has a long standing interest in the antioxidant defense of the eye and has reported the expression and regulation of several redox proteins and GSH in RPE [11,12]. For example, we have presented the evidence for the essential role played by GSH in protection of RPE and retina, and how endogenous protein such as αB crystallin contribute to this process in stressed RPE [12]. In particular, we reported the maintenance of mGSH pool is critical for the health of RPE [7, 12]. Although the transport of mGSH is not fully understood, out of the several mitochondrial membrane carriers, the 2-oxoglutarate (OGC; Slc25a11) and dicarboxylate (DIC; Slc25a10) carriers localized to the inner mitochondrial membrane have been shown to function as GSH transporters in liver, kidney, brain, and colonic epithelial cells [13-16]. Evidence from reconstitution assays in kinetics, proteoliposomes, substrate specificity, dependence on membrane potential and sensitivity to carrier-selective inhibitors indicated a putative role for OGC and DIC in mitochondrial transport of GSH [17].

Moreover, OGC and DIC were identified as the main transporters of cytoplasmic GSH into the renal mitochondrial matrix, and overexpression of either the OGC or the DIC in a renal PT cell line, NRK-52E cells, enhanced mGSH content and protected the cells from cytotoxicity from oxidants and mitochondrial toxicants [16]. The mGSH transport activity exhibited mutual competition with 2-oxoglutarate and sensitivity to phenylsuccinate in HepG2 cells [18]. Furthermore, the transport activity of OGC from rat liver was sensitive to cholesterol-mediated changes in membrane dynamics, thus reproducing the dependence of mGSH transport on membrane fluidity [19].

Despite the available literature on the participation of OGC and DIC in GSH uptake by mitochondria, to our knowledge, there have been no reports on the expression of OGC and DIC in RPE/retina and their role in maintaining mGSH status in retinal health and injury. Accordingly, we investigated the role of mGSH transporters OGC and DIC in RPE cells, and we hypothesized that OGC and/or DIC would be important to the integrity of RPE mitochondria and that inhibition of their carrier activities would lower GSH and lead to functional impairment of mitochondria. Our findings uncover a divergent expression of OGC and DIC in hRPE cells and mouse retina. Selective OGC and DIC downregulation, whose depletion resulted in significant mGSH depletion caused a minimal impact in either whole or cytosolic GSH. Thus, increasing the expression and activity of mGSH transporters OGC and DIC in RPE might be a potential therapeutic target for AMD treatment.

Preprints (www.preprints.org) | NOT PEER-REVIEWED | Posted: 19 July 2018 doi:10.20944/preprints201807.0346.v1

2. Results

2.1 OGC and DIC expression in hRPE cells

To determine whether hRPE cells express OGC and DIC, we used PCR, and Western blot analysis and immunofluorescent staining to evaluate the protein expression of these genes in cultured hRPE cells. We found that both carrier proteins were expressed in hRPE cells (Figure 1A,B). PCR was performed with two specific primer pairs for both OGC and DIC in two human RPE samples, which showed that hRPE cells contained OGC and DIC transcripts (Figure 1A).

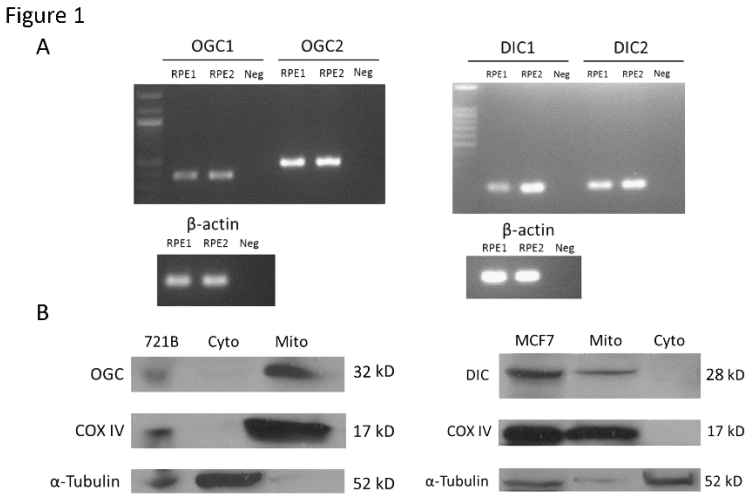

Figure 1. **Gene and protein expression of oxoglutarate carrier (OGC) and dicarboxylate carrier (DIC) in human RPE.** (A), mRNA expression of OGC and DIC in human RPE cells. Reverse-transcription PCR of DIC and OGC was performed using two intron-spanning primer pairs, respectively, for two RPE cDNA from two different donors. RPE1 from donor M; RPE2 from donor N, Neg: negative control. (B), Western blots showing both carriers are expressed in mitochondria of human RPE. Western blot analysis was performed along with positive control cell lysates, 721B (OGC) and MCF7 (DIC). Subunit IV of cytochrome c oxidase (COX IV) was used as the mitochondrial marker, and α-tubulin was used as the cytosolic marker.

To study subcellular localization of OGC and DIC, Western blot analysis was performed in RPE cell lysates along with positive control cell lysates, 721B (OGC) and MCF7 (DIC). As shown in Figure 1B, α-Tubulin (a cytosolic protein marker) was only expressed in cytosolic fractions, was not detectable in mitochondrial fractions. Moreover, COX IV (a mitochondrial protein marker) was only expressed in mitochondrial fractions but not present in cytosolic fractions, demonstrating the purity of the mitochondria fraction isolated from RPE cells (Figure 1B). OGC and DIC were expressed selectively in mitochondria as a ~32 kDa protein (Figure 1B left lanes) and a ~28 kDa protein (Figure 1B right lanes), respectively. Furthermore, we co-stained hRPE cells with Mitotracker Red and OGC and DIC antibodies. The double immunofluorescence staining confirmed that both transporters were co-localized in mitochondria in RPE cells shown in confocal microscope (Figure 2A,B upper lanes) that was consistent with the Western blot analysis. ''No primary antibody'' control is included in Figure 2A,B (bottom lanes). Taken together, these findings firmly establish the mitochondrial localization of OGC and DIC.

 doi:10.20944/preprints201807.0346.v1

117

Figure 2

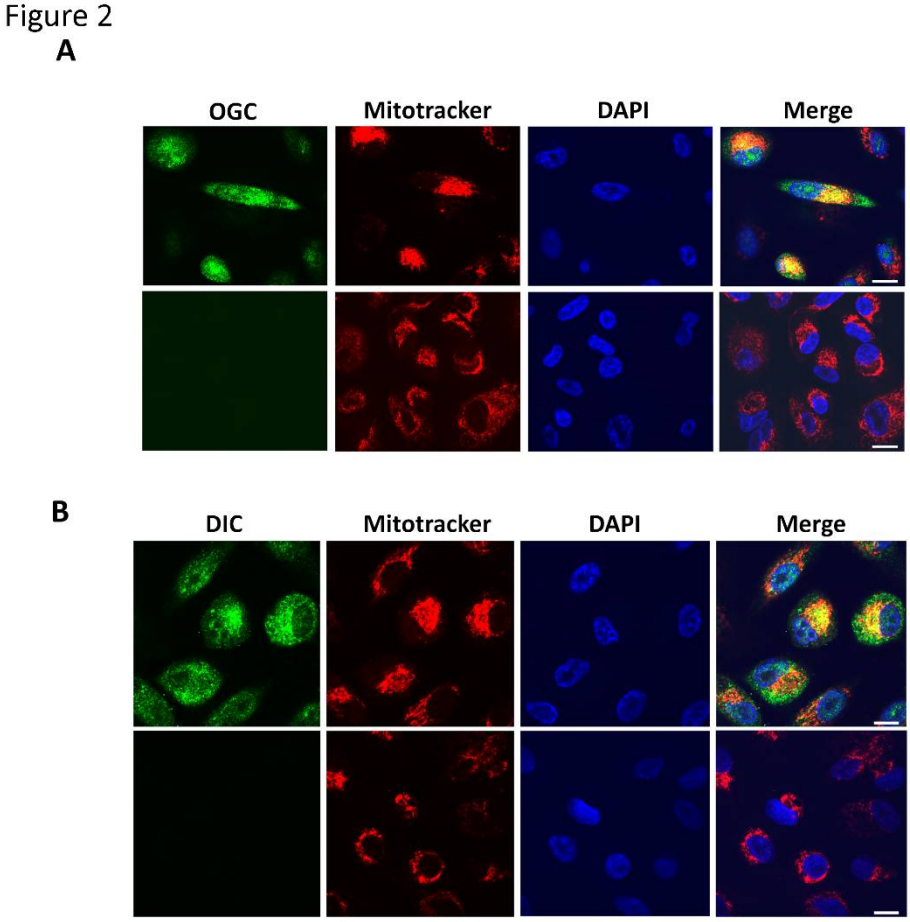

Figure 2. **Confocal images of immunofluorescence staining of OGC and DIC in RPE cells.** (A), (B). OGC and DIC carrier proteins (green) colocalized with mitochondria (Mitotracker, red). DAPI (blue) was used to counterstain nucleus. No primary antibody negative control is shown in lower panels of (A) and (B). Scale bar: 5μm.

118

119

Preprints (www.preprints.org) | NOT PEER-REVIEWED | Posted: 19 July 2018 doi:10.20944/preprints201807.0346.v1

2.2 OGC and DIC expression decreases in hRPE cells under oxidative stress

To gain insight into a potential relevance of OGC and DIC in cellular injury, hRPE cells were subjected to oxidative stress. Oxidative stress from H_2O_2 (50, 100, 200,300 μM for 24 h) caused a dose-dependent decrease of OGC and DIC protein expression (Figure 3A,E). A significant reduction of OGC was observed at higher doses (200 μM and 300 μM) in the H_2O_2-treated group (Figure 3B). As compared to untreated control, OGC also exhibited a time-dependent decrease in expression for up to 24h with a fixed dose of 200 μM H_2O_2, with a 50% decrease occurring as early as 4h (Figure 3C,D). Decreased DIC expression was observed in Western blot analysis as compared to the control group with increasing doses of H_2O_2, especially at 200 μM and 300 μM (Figure 3E,F). Unlike OGC, no time-dependent decrease in DIC expression was observed which remained unchanged up to 24h (Figure 3G,H).

Figure 3

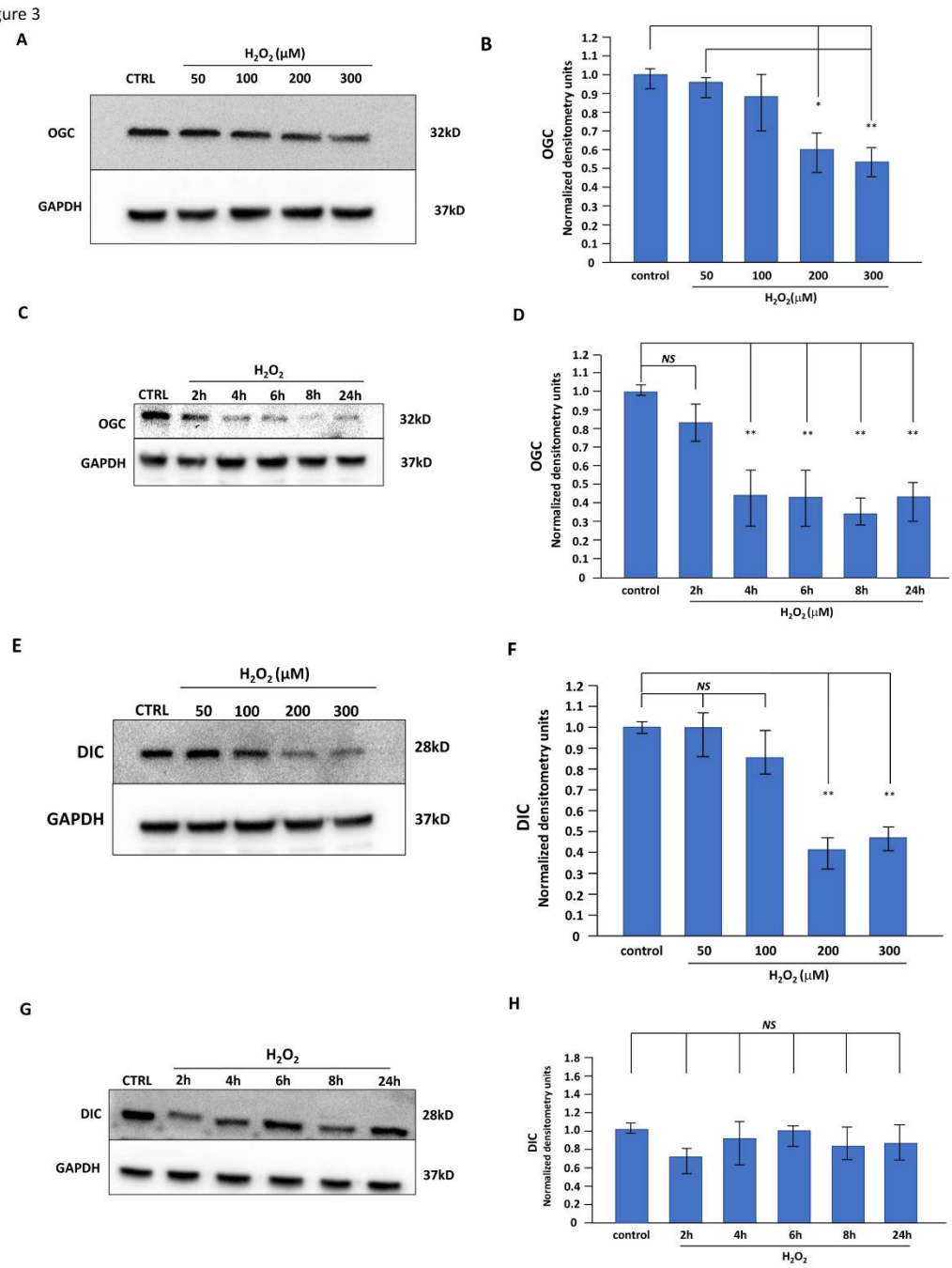

Preprints (www.preprints.org) | NOT PEER-REVIEWED | Posted: 19 July 2018 doi:10.20944/preprints201807.0346.v1

Figure 3. Dose and time dependent changes in OGC and DIC expression in hRPE cells exposed to oxidative stress. hRPE cells were treated with H_2O_2 doses (50µM , 100µM , 200µM,300µM) for 24h (A),(E), and for varying durations (2h,4h,6h,8h, 24h) with 200µM H_2O_2 (C),(G). OGC and DIC proteins were analyzed by Western blot analysis. Quantification of the Western blot shows that both OGC and DIC expression decreased dose dependently with treatment of H_2O_2 compared with untreated control (B),(F). OGC expression decreased significantly with time (P<0.01 vs control) with 200µM H_2O_2 (D), and this trend was not observed in DIC (H). Data are mean ± SEM; n =3,*P<0.05 or **P<0.01, NS: not significant.

2.3 Dose dependent inhibition of OGC and DIC by chemical inhibitors

To validate the relevance of OGC and DIC in RPE, the effect of chemical inhibitors, phenylsuccinate (PS), an inhibitor of OGC, and butylmalonic acid (BM), an inhibitor of DIC was studied. Time and dose-dependency of OGC and DIC protein expression were evaluated in hRPE cells in the presence of the chemical inhibitors. Exposure to three different concentrations (2, 5, 10 mM) of PS and BM, respectively for 24h, caused a significant depletion and dose-dependent down-regulation of OGC and DIC expression during the treatment period (Figure 4A,C). In particular, higher dose of PS and BM (10 mM) induced significantly decreased OGC and DIC protein expression, up to 50% decrease over control, respectively (Figure 4B).

Figure 4

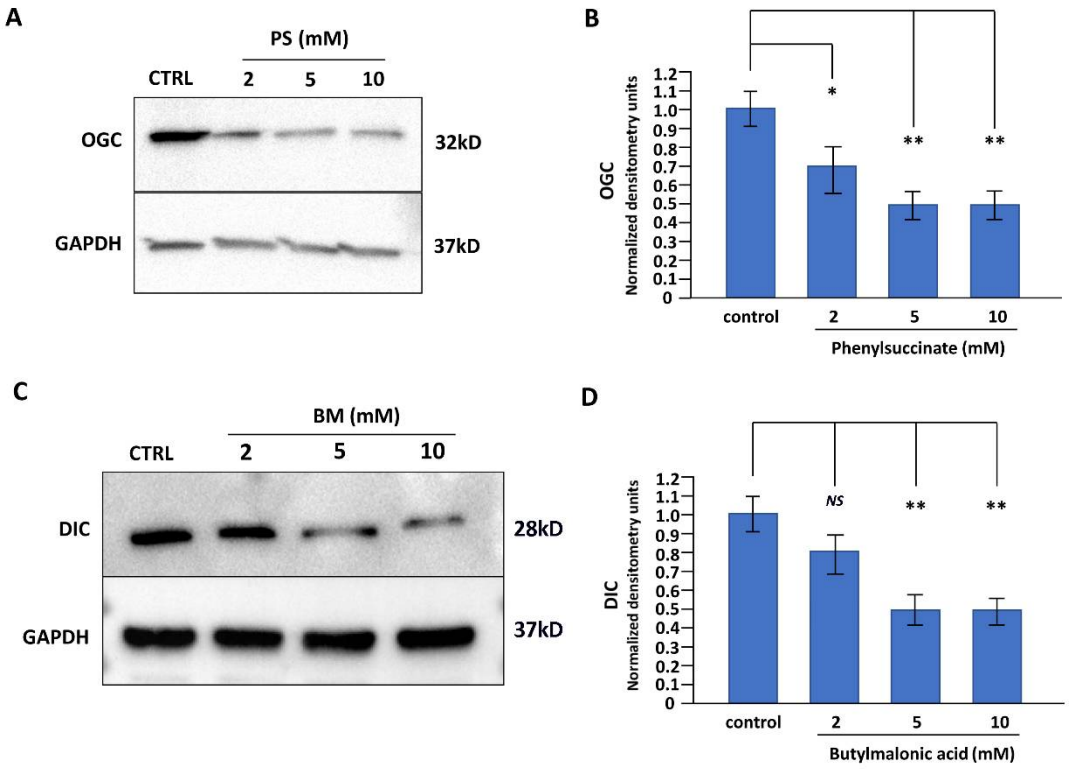

Figure 4. Dose dependent inhibition of OGC and DIC expression by chemical inhibitors. hRPE cells were incubated with PS and BM, the chemical inhibitors of OGC and DIC respectively, at varying doses (2 ,5, 10 mM) for 24h. Western blot analysis shows that the chemical inhibitors caused a depletion of OGC and DIC expression, especially at higher doses. Upper panels show representative gels while lower panels show fold changes calculated by normalization of band density with GAPDH from three independent experiments. Data are mean ± SEM.*, P<0.05 or **, P<0.01. NS: not significant. PS (Phenylsuccinate, inhibitor of OGC); BM (Butylmalonic acid, inhibitor of DIC).

Preprints (www.preprints.org) | NOT PEER-REVIEWED | Posted: 19 July 2018 doi:10.20944/preprints201807.0346.v1

2.4 Glutathione monoethyl ester protects against cell apoptosis induced by OGC and DIC inhibitors

Next, the apoptotic effect of inhibitors of OGC and DIC in hRPE cells was analyzed via TUNEL assay as shown on Figure 5A,C. We quantified the TUNEL positive cells and quantification is presented as fold changes which is the ratio of TUNEL positive cells to the total cells in control group of either the PS (5 mM) or BM (5 mM) treatment groups, with or without GSH-MEE (2 mM). We found that both PS and BM significantly increased TUNEL positive cells as compared to the control group, PS and BM treatment caused a 4.3-fold increase control (7.3-fold vs 1.7-fold, $P<0.0001$) (Figure 5A), and 3.5-fold over control (6.0-fold vs 1.7-fold, $P < 0.0001$) (Figure 5C), in TUNEL assay respectively.

Glutathione monoethyl ester (GSH-MEE) has been shown to protect against oxidative stress and oxidant-induced cell death [13,20]. Therefore, we investigated the effects of cotreatment with GSH-MEE on inhibitor-induced apoptosis in RPE (Figure 5A,C). Cells were treated in medium containing 2 mM GSH-MEE with either PS 5 mM or BM 5 mM (GSH-MEE+PS; GSH-MEE+BM). After 24h treatment, the apoptotic cells detected by the TUNEL assay were significantly decreased in GSH-MEE co-treatment groups compared to the inhibitor-only treatment groups, ($P<0.0001$) (Figure 5B,D). The results indicated that GSH-MEE markedly inhibited apoptosis by reducing cells undergoing apoptosis, and demonstrated the protective effects of GSH-MEE in RPE cells in vitro as a result of reduced apoptosis. We used H_2O_2 treatment with a fixed dose (200 μM) as a positive control (data not shown).

Figure 5

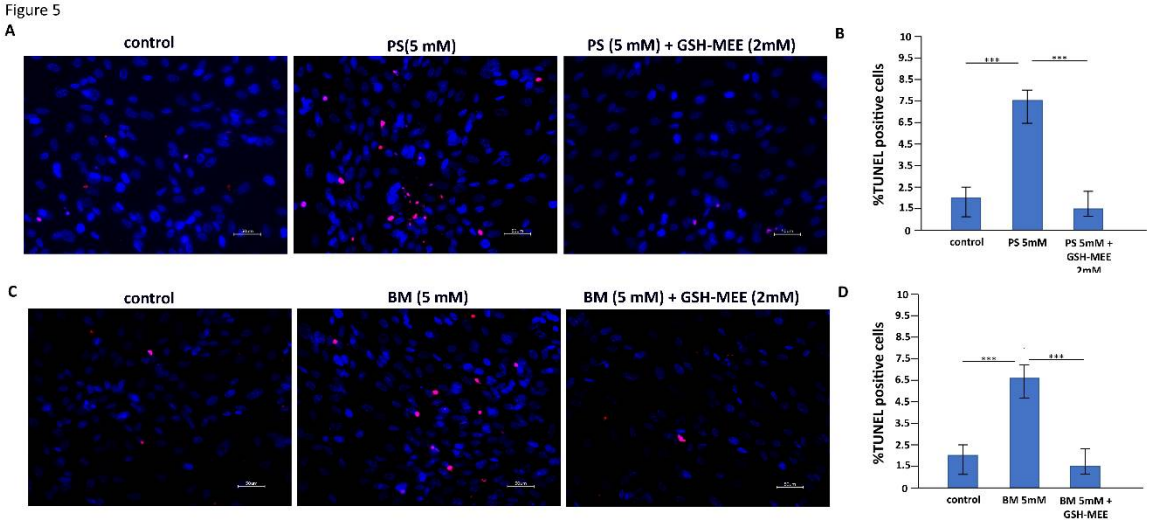

Figure 5. **Induction of apoptosis by OGC and DIC inhibitors and suppression by GSH-MEE.** (A),(C). hRPE cells were treated with a single 5mM dose of either PS or BM with or without GSH-MEE (2mM) cotreatment for 24 h, cell death was determined by TUNEL staining (red). Nuclei were stained with DAPI (blue). Cell death was significantly higher in PS and BM treated cells than in cells cotreated with GSH-MEE. (B),(D). Quantification of the TUNEL-positive cells. Cotreatment with GSH-MEE significantly inhibited cell apoptosis induced by OGC and DIC inhibitors. Data are mean ± SEM from three independent experiments performed in duplicate. *P<0.05 or ** P<0.01, *** P<0.001. NS: not significant. GSH-MEE, GSH monoethyl ester.

2.5 Time-dependent kinetics of caspase 3/7 activation with OGC and DIC inhibitors and its suppression by GSH-MEE

To confirm the induction of apoptosis with OGC and DIC inhibitors, and the attenuation of cell death by GSH-MEE, live cell imaging was performed using the IncuCyte ZOOM and fluorescence microscopy. The kinetics of cell death induced by OGC and DIC inhibitors and suppression by

 doi:10.20944/preprints201807.0346.v1

GSH-MEE were evaluated by IncuCyte live cell analysis, according to the protocol supplied by the manufacturer. The IncuCyte system allows for real time monitoring of cell apoptosis by determining the number of caspase 3/7 positive cells (green fluorescent labeling) at various treatment intervals (Figure 6). Cells undergoing apoptosis with treatments at 6h were stained with SYTOX Green dye, and is shown in Figure 6C. Cells were cultured in 1% FBS containing medium and stimulated with 5 mM PS (Figure 6A green), 5 mM BM (Figure 6A yellow), PS+ GSH-MEE (Figure 6A blue), BM +GSH-MEE (Figure 6A grey), respectively. Activation of caspase-3/7 generation increased in a time-dependent manner in both PS and BM treatment groups (Figure 6A green and yellow), with peak cell death up to 50 fold over the control condition achieved in 6 h (Figure 6C), which indicated that the apoptosis induced by the inhibition of OGC and DIC is associated with a rapid cell death in RPE cells, with time to peak reached within a few hours. In addition, we tested GSH-MEE co-treatment, which resulted in significant reduction of apoptosis triggered by the inhibitors ($P<0.0001$) (Figure 6A grey and blue), that was consistent with the findings of the TUNEL assay. Compared with PS and BM treatment groups, (PS+GSH-MEE) and (BM+GSH-MEE) groups showed a significant reduction in apoptosis, respectively, indicating that GSH-MEE could rescue cells from the injury caused by OGC and DIC inhibitors. Overall, these results highlight the apoptotic effects of the inhibitors of OGC and DIC, and the antiapoptotic effects of GSH-MEE in hRPE cells.

Preprints (www.preprints.org) | NOT PEER-REVIEWED | Posted: 19 July 2018 doi:10.20944/preprints201807.0346.v1

Figure 6

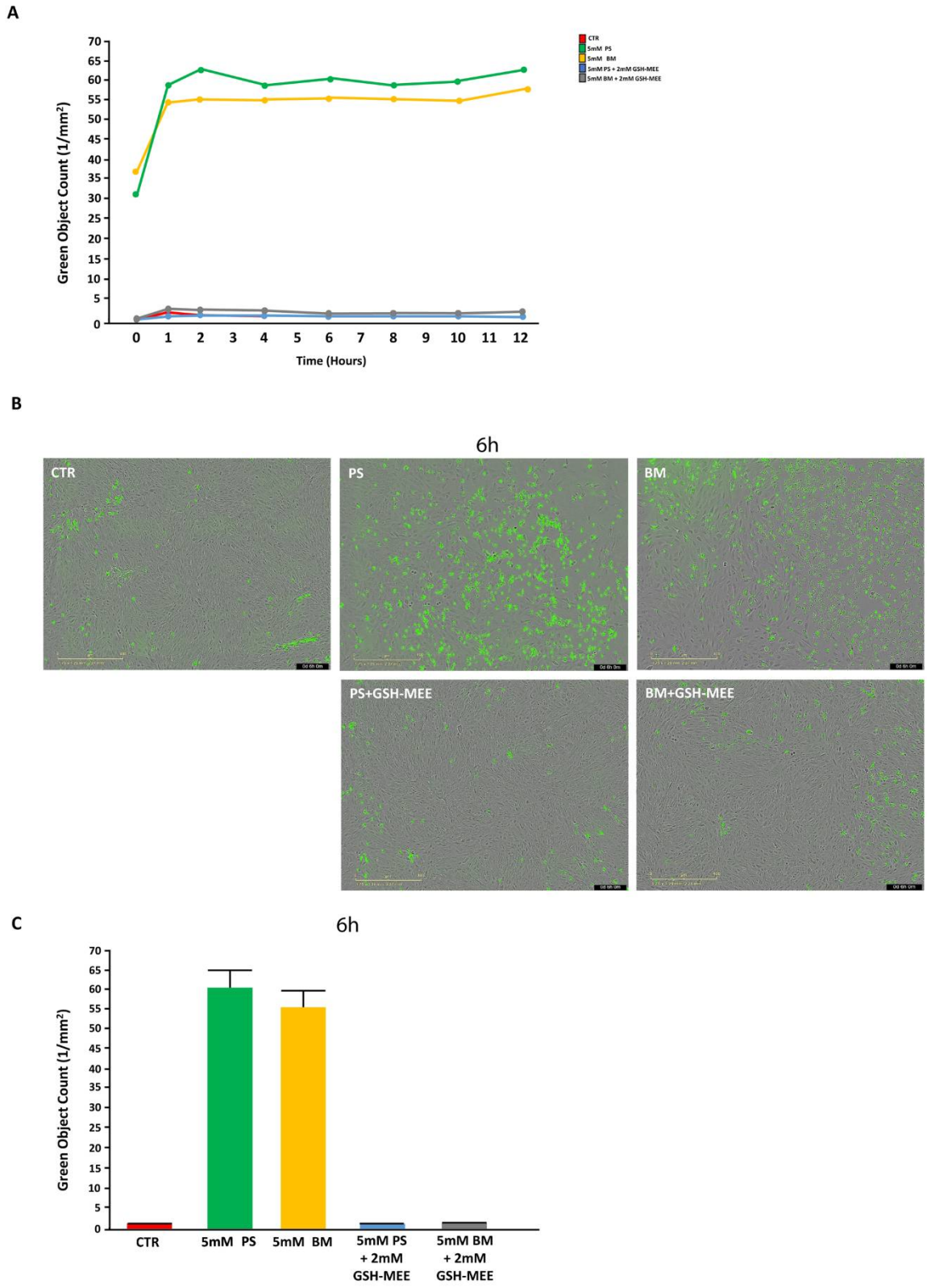

 doi:10.20944/preprints201807.0346.v1

Figure 6. Time dependent increase in caspase-3/7 generation with OGC and DIC inhibitors and suppression by GSH-MEE. (A). Kinetic measure of the number of caspase 3/7 positive cells was over time in response to specified treatments. hRPE cells were plated and either left unstimulated or stimulated with 5 mM PS (green) , 5 mM BM (yellow), or cotreated with 2 mM GSH-MEE (PS+GSH-MEE: blue and BM+GSH-MEE: grey). Images were acquired every 15 min. Automated real-time assessment by IncuCyte ZOOM, measured as green object count for all cells stained green with SYTOX Green, which was allowed to generate graphics of the data as soon as image analysis was complete. PS and BM induced significant cell apoptosis compared with its control, which was suppressed by GSH-MEE. (A). Caspase-3/7 activation increased for the first two h with PS and BM which was inhibited by cotreatment with GSH-MEE. (B). IncuCyte ZOOM image (phase contrast and green fluorescence overlaid) of hRPE cells with stimulus at 6 h. Cells undergoing apoptosis have membrane compromise, and their DNA are stained with SYTOX Green dye that is already present in the media along with the stimuli (original magnification X20). (C). Quantification of the activation of caspase-3/7 (green fluorescent staining of nuclear DNA) at 6 h in the treatment groups showing the suppression of inhibitor-induced caspase-3/7 activation by GSH-MEE. H_2O_2 treatment of RPE cells was used as a positive control. Data are shown as mean ± SEM (n=4).

188

189 *2.6 GSH-MEE supplementation attenuates inhibitor-induced depletion of mGSH in hRPE cells*

190 Next, we sought to investigate whether the inhibitor induced cell death is a result of decreased
191 antioxidant defense as evidenced by changes in glutathione (GSH). GSH levels were measured in
192 whole cell, and the isolated cytosolic and mitochondrial fractions from RPE cells, after 24h
193 treatment with either 5 mM PS or BM, in the presence or absence of 2 mM GSH-MEE. The results
194 show that there was no significant difference in GSH levels either in whole cell lysates (Figure 7A,B)
195 or the cytosolic fractions (Figure 7C,D), in the treatment groups. On the other hand, the
196 concentration of mGSH exhibited significant differences among the treatment groups (Figure 7E,F).
197 As shown in Figure 7E, mGSH level was 0.6-fold lower in PS treatment group than that in control
198 group ($P<0.05$), and BM treatment also induced 0.7-fold depletion of mGSH level compared to
199 control condition ($P<0.05$) (Figure 7F). It indicates that the inhibitors of OGC and DIC significantly
200 deplete the GSH level in mitochondria, but have little effect on whole cell and cytosolic GSH. These
201 results are consistent with the known increase in ROS and a pro-oxidative environment in OGC and
202 DIC-deficient cells.

203 Earlier studies have provided evidence indicating that GSH-MEE freely crosses membrane
204 bilayers and diffuses into mitochondria, contributes to mGSH replenishment, and protects against
205 oxidative stress in several cell types [21-23]. Therefore, we determined whether GSH-MEE
206 treatment attenuated inhibitor-induced depletion of mGSH concentration in hRPE cells. The results
207 showed that GSH level was approximately three-fold elevated in (PS+GSH-MEE) group over PS
208 group ($P<0.01$) (Figure 7E). Similar replenishment of mGSH by GSH-MEE was observed in
209 (BM+GSH-MEE) treatment group, four-fold increase of mGSH compared to BM group (Figure 7E,
210 right lane). Interestingly, the restoration of mGSH level was higher than that of control GSH,
211 indicating that additional mitochondrial mechanisms may exist for this phenomenon. In general, as
212 we expected, GSH-MEE co-treatment was able to rapidly enhance mGSH levels in both PS and BM
213 treatment groups (Figure 7E,F), but had little effect in whole cell and cytosolic GSH (Figure 7A-D),
214 suggesting that GSH-MEE would represent an effective tool to specifically elevate the mGSH pool
215 under the inhibition of OGC and DIC in hRPE cells.

Preprints (www.preprints.org) | NOT PEER-REVIEWED | Posted: 19 July 2018 doi:10.20944/preprints201807.0346.v1

Figure 7

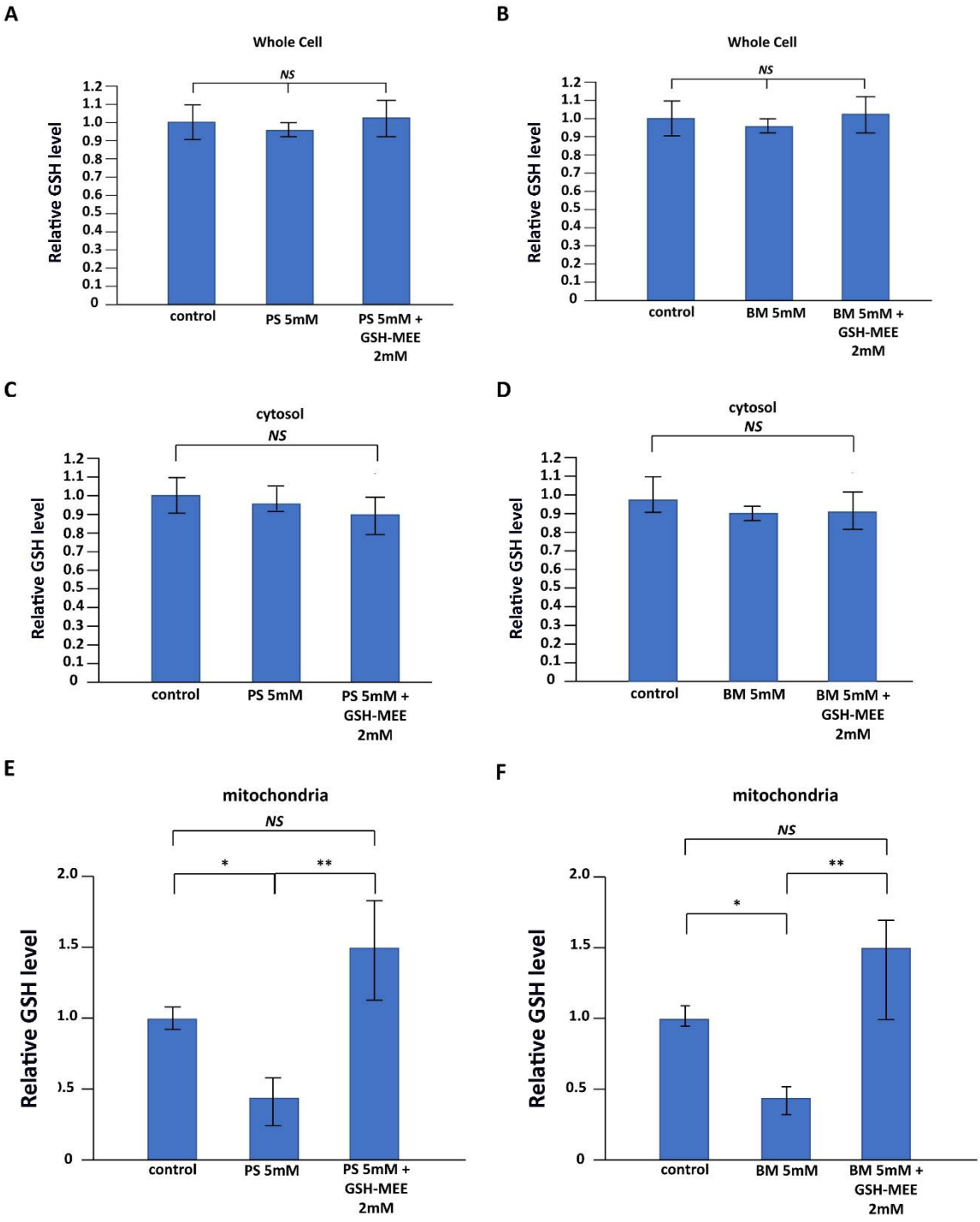

216

Figure 7. Selective depletion of mitochondrial GSH level with OGC and DIC inhibitors and repletion with GSH-MEE co-treatment. GSH levels were measured in whole cell lysates (A),(B), cytosolic fraction (E),(F), mitochondrial fraction (C),(D). (C),(D) show GSH levels were significantly decreased with inhibitors but is restored to above control levels with GSH-MEE. Whole cell and cytosolic fractions do not show such a change (E),(F). The GSH levels were normalized to control level (=1). All experiments were carried out in triplicate. Data are shown as mean ± SEM of three independent experiments, *P<0.05 or ** P<0.01, *** P<0.001, NS: not significant. GSH-MEE, GSH monoethyl ester.

 doi:10.20944/preprints201807.0346.v1

2.7 Effect of polarity on OGC and DIC expression

We investigated the effect of polarization of hRPE cells on the expression of OGC and DIC, and compared polarized RPE to that of non-polarized RPE cells. The polarization of the RPE cells was confirmed by their transepithelial electrical resistance (TER = 160 ± 57.1 Ω·cm²). As shown in Figure 8, OGC and DIC protein expression was significantly increased in polarized RPE cells than that in non-polarized RPE cells (1.4-fold vs non polarized; P<0.01).

Figure 8

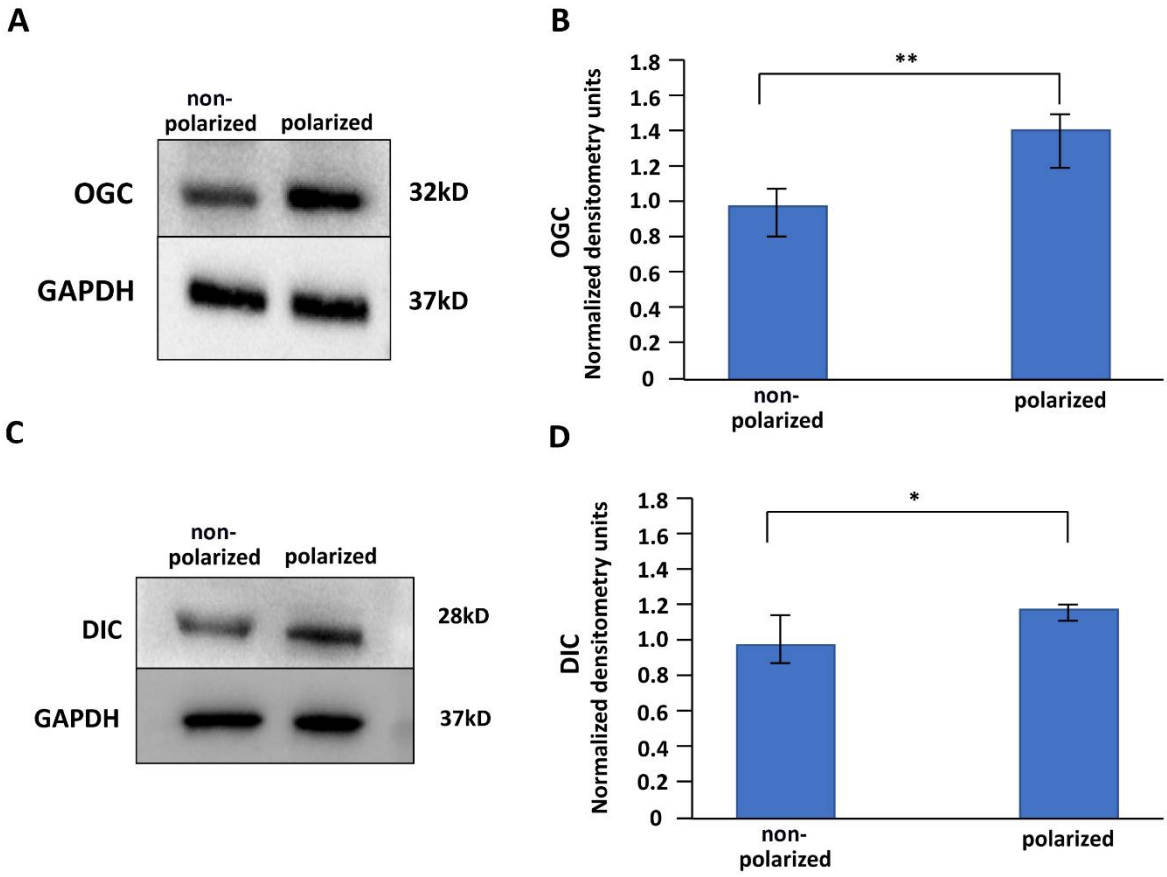

Figure 8. Effect of polarity on OGC and DIC expression in hRPE cells. Western Blot analysis was performed in lysates from confluent non-polarized and polarized RPE cells, gel images (left) and bar graphs (right) analyzed from three independent experiments. Data are shown as mean ± SEM, the mean TER of polarized cells was 160 ± 57.1 Ω·cm². ** P<0.01, *** P<0.001.

 doi:10.20944/preprints201807.0346.v1

2.8 Localization of OGC and DIC in mouse retina

To determine the distribution of OGC and DIC in the mouse retina, especially in the RPE and choroid layer, immunostaining was used. OGC and DIC expression was evident by a strong green fluorescence in the photoreceptor inner segments, which harbor abundant mitochondria. Immunofluorescent labeling in mouse retinas with OGC and DIC antibodies showed clear evidence for localization of the two transporters in the inner segments (IS) and photoreceptors (Figure 9). ''No primary antibody'' control was also included in this analysis (Figure 9A, bottom lanes).

Next, in order to measure the expression of OGC and DIC in retinal tissue, mitochondrial and cytosolic fractions were isolated from RPE and choroid segments of 129-S6/SvEvTac mice retina. The purity of the fresh isolated mitochondria was evaluated by Western blot analysis. As in the case of hRPE (Figure 1), α-Tubulin was used as a cytosolic protein marker, and COX IV was used as a mitochondrial protein marker. The results revealed that the isolated mitochondria from RPE/choroid section was pure. The results from Figure 9A show that both OGC and DIC were expressed in the mitochondrial fraction of RPE/choroid, but only negligibly in the cytosolic fraction, which is consistent with the findings of selective mitochondrial expression in cultured hRPE cells (Figures 1,2).

 doi:10.20944/preprints201807.0346.v1

Figure 9

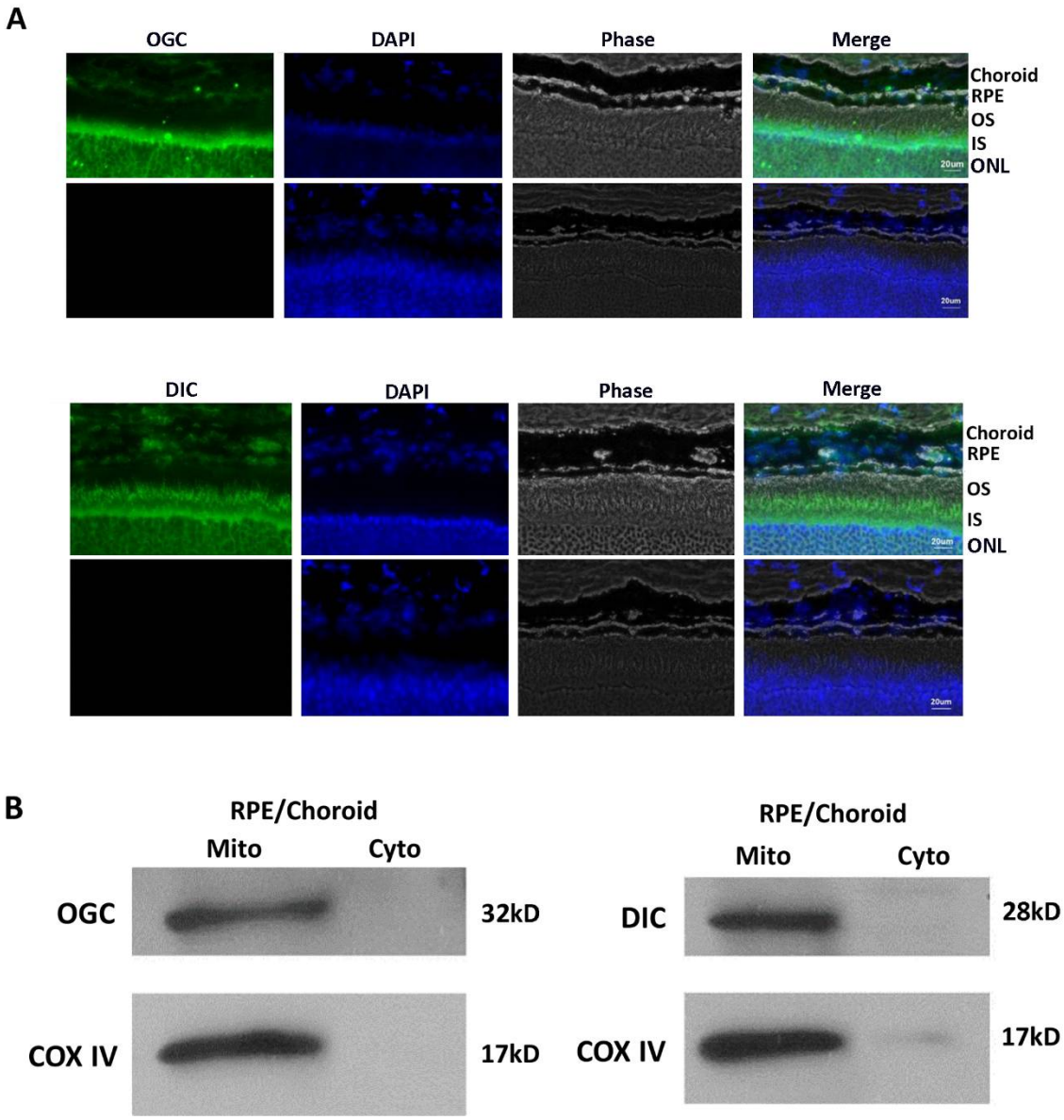

242

Figure 9. **Expression of OGC and DIC (green) in mouse retinal layers in mouse RPE/choroid.** (A). Immunofluorescence staining of OGC and DIC (green) of the posterior eye cup of mice. DAPI (blue) was used to counterstain nuclei. Upper panels diffuse green fluorescence can be seen in RPE. Strong green fluorescence was noted at the photoreceptor inner segment which harbor abundant mitochondria. Bottom panels show negative control devoid of primary antibody for OGC and DIC. Scale bar 20 μm. (B). Protein expression of OGC and DIC in RPE/choroid of mice. Mitochondrial and cytosolic fractions of RPE/choroid from mice were isolated and immunoblotted for DIC and OGC. Both carriers are expressed in mitochondrial fraction of RPE/choroid and are absent in the cytosol. OS: Photoreceptor outer segments; IS: Photoreceptor inner segments; ONL: outer nuclear layer. RPE: Retinal pigment epithelium layer.

 doi:10.20944/preprints201807.0346.v1

3. Discussion

We have gathered data on the characterization of mitochondrial uptake of GSH in RPE cells and have presented evidence for the regulation of uptake by oxidative stress. The characterization and selective localization of OGC and DIC (two solute carrier proteins of the SLC25A family) in RPE cells and their expression in mouse retinal layers has been made for the first time. The significance of mGSH for normal RPE function was further verified by augmentation of apoptotic cell death with chemical inhibition of OGC and DIC and prevention of cell death by co-incubation with GSH-MEE.

Mitochondria play an important role in formation of energy, reaction oxygen species and cell death due to apoptosis. Damage to mitochondria with oxidative, environmental, and genetic factors can lead to damage to mitochondrial DNA. Evidence implicates mitochondrial damage in the AMD disease process [24,25]. Ferrington's laboratory found a potential link between mitochondrial dysfunction due to increased mitochondrial DNA lesions and AMD [26-28]. Thus, protecting mitochondrial DNA integrity via therapeutics targeted to the mitochondria early in AMD could stop or ameliorate the progression to vision loss.

Mitochondria possess several detoxifying enzymes and antioxidants such as MnSOD, glutaredoxin and GSH. GSH forms a sizable pool in the mitochondrial compartment and the role of GSH in retinal neuroprotection is well known. Unlike cytosol, mitochondria do not synthesize GSH de novo from its constituent amino acids and mGSH originates from the transport of cytosolic GSH into mitochondria by a carrier-specific process exhibiting dual kinetic components [29]. As mentioned previously, we and others have shown that mGSH plays a key role in the removal of ROS in injured RPE [12,30]. Since GSH is negatively charged and is unable to pass freely across the lipid bilayer, both outer and inner mitochondrial membranes must harbor transporters or channels that facilitate entry of GSH into mitochondria [10]. In the current study, we have identified OGC and DIC as the two solute carrier proteins that mediate the uptake of GSH by RPE mitochondria. These two proteins are members of the SLC25 transporter family and vary greatly in the nature and size of the transported substrates, modes of transport and driving forces although the mechanism of substrate translocation may not differ [31]. We could establish that both proteins are expressed selectively in mitochondria of human RPE cells as well as in RPE/choroid of young mouse retina. A wide body of data suggests that these transporters reside in the inner mitochondrial membrane in several cell lines and tissues and mediate GSH import to mitochondria [15,16, 29, 32, 33]. OGC mediated transport was not found in bacteria [34], contrasting the functional expression of mitochondria-targeted OGC from HepG2 transport in Xenopus oocytes and the reconstitution of partially purified OGC in proteoliposomes from kidney mitoplasts [35,36]. Thus the findings from Booty et al. [34] may arise from biochemical and biophysical properties of L. Lactis or OGC or OGC may require other partners under their experimental conditions [19].

We found that inhibition of OGC and DIC sensitized RPE cells to apoptosis. Live-cell imaging of caspase 3/7 activation established that the induction of apoptosis is rapid and occurs as early as 2h (Figure 6). Under these conditions, mGSH is decreased significantly while whole cell and cytosolic GSH remained unaltered. Our studies also revealed that the decrease in GSH and induction of apoptosis could be overcome by co-incubation with GSH-MEE indicating the significance of OGC and DIC in maintaining proper RPE function. It will be interesting to establish the correlation of OGC/DIC depletion with mitochondrial function such as ATP generation and respiratory complex proteins and restoration of GSH levels by known GSH replenishing agents.

Our laboratory has shown that the expression of growth factors can be regulated by the polarity of the RPE [37-39]. For example, we have shown that amount of secretion of PEDF varies several folds based on the polarity of human RPE in the order: non-polarized<polarized <stem cell RPE [37]. Consistent with this, we found that both OGC and DIC expression increased in polarized RPE as compared to non-polarized RPE making polarized RPE more resistant to oxidative injury.

 doi:10.20944/preprints201807.0346.v1

In addition to establishing the expression and localization of OGC and DIC, we have documented their expression in RPE/choroid and in the inner nuclear layer of the mouse retina. These experiments suggest that OGC and DIC may also contribute to the health of photoreceptors and the neural retina, though additional supportive evidence using astroglial cells and Muller cells will be necessary to confirm this hypothesis. It is hoped that the information presented here will be of use in studies on the expression of mGSH transporters in pathophysiological mouse models and in devising strategies for restoring mitochondrial and cellular integrity through increasing GSH status

4. Materials and Methods

4.1 Cell culture

All experiments and procedures were conducted in compliance with the Declaration of Helsinki. The RPE cells were isolated from human fetal eyes as previously described [40]. Confluent cell cultures from passages 2 to 4 were used. The cells were cultured in Dulbecco's modified Eagle medium (DMEM, Fisher Scientific, Pittsburgh, PA, USA) with 2 mM L-glutamine, 1% Antibiotic-Antimycotic (Gibco life technologies, Carlsbad, CA) and 10% fetal bovine serum (FBS; Laguna scientific, CA) at 37°C under 5% CO_2. Highly differentiated polarized RPE were cultured on Transwell filters for 1 day in 10% FBS containing medium and in 1% FBS thereafter for 4 weeks. The TER of the RPE cells on the Transwells filters was measured with the Epithelial Voltohmmeter 2 (EVOM2; World Precision Instruments, Sarasota, FL) as described before [40]. MCF7 cell lysates (Manassas, VA, USA) were used as positive control for OGC and 721_B cell lysates (Aviva, Systems Biology) were used as positive control for DIC.

4.2 Cell Exposures

The RPE cell culture medium was switched to FBS-free medium overnight to minimize the effect of serum. To study the effect of H_2O_2 on expression of OGC and DIC, the cells were exposed to H2O2 at varying doses (50 μM, 100 μM, 200 μM, 300 μM) for 24h, and varying durations (2h, 4h, 6h, 8h, 24h) with 200 μM H_2O_2. To identify dose dependent inhibition of OGC and DIC expression by chemical inhibitors, cells were incubated with Phenylsuccinic acid (PS; Sigma-Aldrich, St Louis, MO) and Butylmalonic acid (BM; Sigma-Aldrich, St Louis, MO) in varying doses (2 mM ,5 mM, 10 mM) for 24h, respectively. Cells were also treated with a single dose 5 mM of either PS or BM, with or without 2 mM GSH-MEE (Santa Cruz biotechnology, CA) treatment for 24 h. In the experiments with inhibitors, control cells were treated with serum-free medium containing 0.1% dimethyl sulfoxide (DMSO).

4.3 Western blot analysis

Protein was extracted from the cells using RIPA buffer (Cell Signaling Technology, Danvers, MA) and determined by a protein assay kit (Bio-Rad; Hercules, CA) using bovine serum albumin as the standard. Equal amounts of proteins (30 μg/well) were resolved on 8–16% polyacrylamide gel and transferred to PVDF blotting membranes (Millipore, Billerica, MA). Membranes were probed overnight at 4°C with primary antibody, anti-OGC rabbit polyclonal antibody (1:1000) and anti-DIC rabbit polyclonal antibody (1:1000), anti-COX IV (1:1000), anti-α-tubulin (1:3000). After incubation with the appropriate secondary antibody to rabbit IgG or to anti-mouse (Vector Laboratories), protein bands were detected by an enhanced chemiluminescence (ECL) detection system (Thermo Scientific, Rockford, IL). To verify equal loading, membranes were reprobed with GAPDH. 721B cell lysates was used as positive control for OGC and MCF7 cell lysates was used as positive control for DIC. Subunit IV of cytochrome c oxidase (COX IV) and α-tubulin were used as the mitochondrial marker and cytosolic marker, respectively.

4.4 Reverse Transcriptase Polymerase Chain Reaction

 doi:10.20944/preprints201807.0346.v1

Total RNA was extracted from confluent hRPE cells using RNeasy Mini Kit (Qiagen, Valencia, CA). One microgram of total RNA was used for cDNA synthesis using the First-Strand cDNA Synthesis Kit (Invitrogen) according to the manufacturer's instuctions. PCR was performed using HiFidelity Polymerase Kit (Qiagen), and β -Actin served as the internal control. The PCR primers used (Valuegene Inc, San Diego, CA) were from published sequences. Results were reported as fold change over controls.

4.5 Localization of OGC and DIC in RPE Cells by immunofluorescence

Confluent RPE cells were grown in four-well chamber slides (Falcon, Corning, NY). To visualize the mitochondria, Mitotracker Red CMXRos (500nM; Life Technologies, Carlsbad, CA, USA) was added to samples and incubated at 37 ℃ for 10 min, prior to fixation with 4% paraformaldehyde. Cells were washed with phosphate buffered saline (PBS) and permeabilized in PBS containing 0.5% Triton X-100 for 30 min, and then blocked in 5% normal goat serum for 30 min. Primary antibodies, anti-OGC (1:100, Abcam, Cambridge, MA); anti- DIC (1:100, GeneTex, Irvine, CA) were added to cells incubated at 4°C overnight. An anti-rabbit fluorescence-conjugated secondary antibody (Vector Laboratories, Burlingame, CA) was used for 30 min in the dark at room temperature. After nuclear staining with DAPI (Vector Labs, Burlingame, CA), the slides were examined on an LSM 710 laser-scanning microscope (Carl Zeiss).

4.6 TUNEL Staining

Apoptosis was detected by the terminal deoxynucleotidyl transferase (TdT)-mediated dUTP-biotin nick end-labeling (TUNEL) method according to the manufacturer's protocol (In Situ Cell Death Detection Kit; Roche Applied Science, Indianapolis, IN, USA). Briefly, RPE cells were treated with inhibitors, with the presence or absence of GSH-MEE. H_2O_2 (200 μM) was used to as a positive control. After fixing with 4% PFA solution and permeabilized with 0.5% Triton X-100, the cells were incubated with TUNEL reaction mixture at 37°C for 1 h in a humidified chamber. After the TUNEL reaction, cells were counterstained with DAPI and then directly analyzed using fluorescence microscopy (Keyence, Itasca, IL). The number of TUNEL-positive cells in 10 randomly selected microscopic fields (40x) was counted in a masked fashion.

4.7 IncuCyte cell apoptosis assay

To evaluate the inhibitors of OGC and DIC effects on cell apoptosis, RPE cells (5,500 cells/well) were plated in 96-well plates (Corning, NY). The treatment reagents were added to each well already containing SYTOX Green dye caspase 3/7 reagent diluted in cell culture media (1:1000 dilution) to make a total volume of 100 μl/well. Each condition was run in five replicate wells. The following four groups were used in total analysis: control, PS, BM, PS+GSH-MEE, BM+GSH-MEE. H_2O_2 treated cells served a positive control. Cell apoptosis was monitored for 24 h using the IncuCyte ZOOM system (Essen Bioscience, Ann Arbor, MI, USA), which allows an automated in-incubator method of monitoring live cells. Green (400-ms exposure) channels in the IncuCyte ZOOM platform, which is housed inside a cell incubator at 37°C with 5% CO_2. Four image sets from distinct regions per well were taken every 30 min. Automated real-time assessment by IncuCyte ZOOM, measured as green object count for all cells stained green with SYTOX Green, which was allowed to generate graphics of the data as soon as image analysis was complete. Graphics were generated with IncuCyte Basic Software graph/export functions.

4.8 Preparation of mitochondrial and cytosolic fractions

Cells were harvested after the specified experimental period and total cellular protein was extracted. Mitochondrial and cytosolic proteins were isolated by using a commercial Mitochondria/Cytosol Fractionation Kit following manufacturer's protocol (BioVision Inc., Mountain View, CA). Mitochondria were isolated from the freshly collected cells according to the method described previously. Briefly, RPE cells (5×10^7 cells per sample) were harvested by centrifugation at

 doi:10.20944/preprints201807.0346.v1

600 ×g for 5 min at 4°C, cells washed with 10ml ice-cold PBS, centrifuged at 600 ×g for 5 min at 4°C to remove nuclei and unbroken cells, this was followed by resuspension of cells with 1.0 ml 1 ×Cytosol extraction buffer mix containing DTT and protease inhibitors, and incubation on ice for 10 min, and homogenization in a Dounce tissue grinder on ice. The homogenate was centrifuged at 700x g for 10 min to remove cellular debris and then at 10,000xg for 30 min to pellet the mitochondria. The supernatant was collected as the cytosol portion while the mitochondrial fraction tube was resuspended in 150 µl of mitochondrial buffer. Samples were measured immediately for GSH content as described below.

4.9 Assay for GSH content

The samples were loaded to 96-well plates, and the total cellular, mitochondrial and cytosolic GSH were measured as described before [5] by using a glutathione assay kit (BioVision, Mountain View, CA) following the manufacturer's protocol. GSH react to generate 2-nitro-5-thiobenzoic acid, the reaction products which has yellow color determined by measuring absorbance at 405 nm using a microplate reader (Bio-Rad, CA). Total GSH levels were calculated by using a standard curve generated in parallel experiments, expressed as µg/10^6 cells and were normalized to percent of control. GSH measurements were obtained from at least three independent experiments.

4.10 Localization of OGC and DIC in mouse retinal layers by immunofluorescence

129-S6/SvEvTac mice were purchased from Taconic Farms (Germantown, NY) and eye cups were prepared as described [41]. Cryosections at 10-µm thick were cut and collected for immunochemistry procedure by using either rabbit antibody against OGC (1:100) or rabbit antibody against DIC (1:100) overnight at 4°C. After incubation with primary antibodies, the sections were washed and incubated with appropriate secondary antibody. Negative control sections were incubated with blocking buffer without primary antibody and then processed as described above. The sections were photographed with a confocal laser microscope (LSM 710, Carl Zeiss).

4.11 Statistical analysis

All data were expressed as mean± S.E.M. Statistical analysis was performed using ANOVA followed by Tukey post-test using software GraphPad Prism(Version 5, GraphPad Software, Inc., La Jolla, CA).$P < 0.05$ was considered significant.

5. Conclusions

In this work, we have characterized the expression of OGC and DIC in hRPE cells and mouse retina, and have shown that their inhibition results in depletion of mGSH. This finding indicates that OGC and DIC carrier protein expression is important for mitochondrial antioxidant defense in RPE cells. Augmenting the mGSH level may prove to be a novel therapeutic approach for AMD.

Author Contributions: R.K., D.R.H., and S.S. conceived and designed the experiments. M.W., L-L., P.G.S., and L.L. performed the experiments and analyzed the data. M.W. and R.K. wrote the manuscript, and C.S. and D.R.H. provided hRPE cells and polarized RPE cells. All authors read and approved the manuscript.

Funding: This work was supported by NIH grants EY01845 and CORE EY03040 and funds from the Arnold and Mabel Beckman Foundation.

Acknowledgments: We sincerely thank Eric and Ernesto Barron for help with live cell imaging analysis and in preparation of figures.

Conflicts of Interest: The authors declare that they have no conflicts of interest..

Abbreviations

AMD	Age-related macular degeneration
GSH	Glutathione
ER	Endoplasmic reticulum

 doi:10.20944/preprints201807.0346.v1

mGSH	Mitochondrial glutathione
ROS	Reactive oxygen species
SLC25A	Solute carrier family 25A
RPE	Retinal pigment epithelium
GSSG	Glutathione disulfide
OGC	2-oxoglutarate carrier
PS	Phenylsuccinate
DIC	Dicarboxylate carrier
BM	Butylmalonate
GSH-MEE	Glutathione monoethyl ester
COX-IV	Cytochrome c Oxidase Subunit IV
TER	Transepithelial electrical resistance

References

1. Ambati J.; Fowler B.J. Mechanisms of age-related macular degeneration. *Neuron* **2012**, *75*, 26-39.
2. Beatty S.; Koh H.; Phil M.; Henson D.; Boulton M. The role of oxidative stress in the pathogenesis of age-related macular degeneration. *Surv Ophthalmol* **2000**, *45*, 115–134.
3. Cai J.; Nelson K.C.; Wu M.; Sternberg P Jr.; Jones D.P. Oxidative damage and protection of the RPE. *Prog Retin Eye Res* **2000**, *19*, 205-21.
4. Brown E.E.; Lewin A.S.; Ash J.D. Mitochondria: Potential Targets for Protection in Age-Related Macular Degeneration. *Adv Exp Med Biol* **2018**, *1074*, 11-17.
5. Wilkins H.M.; Kirchhof D.; Manning E.; Joseph JW.; Linseman D.A. Mitochondrial Glutathione Transport Is a Key Determinant of Neuronal Susceptibility to Oxidative and Nitrosative Stress. *J Biol Chem* **2013**, *288*, 5091–5101.
6. Sternberg P Jr.; Davidson P.C.; Jones D.P.; Hagen T.M.; Reed R.L.; Drews-Botsch C. Protection of retinal pigment epithelium from oxidative injury by glutathione and precursors. *Invest Ophthalmol Vis Sci* **1993**, *34*, 3661-3668.
7. Sreekumar P.G.; Spee C.; Ryan S.J.; Cole S.P.; Kannan R.; Hinton D.R. Mechanism of RPE cell death in α-crystallin deficient mice: a novel and critical role for MRP1-mediated GSH efflux. *PLoS One* **2012,** *7*, e33420.
8. Lu S.C. Glutathione synthesis. *Biochim Biophys Acta* **2013**, *1830*, 3143-53.
9. Ribas V.; García-Ruiz C.; Fernández-Checa J.C. Glutathione and mitochondria. *Front Pharmacol* **2014**, *5*, 151.
10. Marí M.; Morales A.; Colell A.; García-Ruiz C.; Kaplowitz N.; Fernández-Checa JC. Mitochondrial glutathione: features, regulation and role in disease. *Biochim Biophys Acta* **2013**, *1830*, 3317-3328.
11. Sreekumar P.G.; Ding Y.; Ryan S.J.; Kannan R.; Hinton D.R. Regulation of thioredoxin by ceramide in retinal pigment epithelial cells. *Exp Eye Res* **2009**, *88*, 410-7.
12. Dou G.R.; Sreekumar P.G.; Spee C.; He S.K.; Ryan S.J.; Kannan R.; Hinton D.R. Deficiency of αB crystallin augments ER stress-induced apoptosis by enhancing mitochondrial dysfunction. *Free Radic Biol Med* **2012**, *53*, 1111-1122.
13. Torres S.; Matías N.; Baulies A.; Nuñez S.; Alarcon-Vila C.; Martinez L.; Nuño N.; Fernandez A.; Caballeria J.; Levade T.; et al. Mitochondrial GSH replenishment as a potential therapeutic approach for Niemann Pick type C disease, *Redox Biol* **2017**, *11*, 60–72.
14. von Montfort C.; Matias N.; Fernandez A.; Fucho R.; Conde de la Rosa L.; Martinez-Chantar M.L.; Mato J.M.; Machida K.; Tsukamoto H.; Murphy M.P.; et al. Mitochondrial GSH determines the toxic or therapeutic potential of superoxide scavenging in steatohepatitis. *J Hepatol* **2012**, *57*, 852-859.
15. Lash L.H.; Putt D.A.; Matherly L.H. Protection of NRK-52E cells, a rat renal proximal tubular cell line, from chemical-induced apoptosis by overexpression of a mitochondrial glutathione transporter. *J Pharmacol Exp Ther* **2002**, *303*, 476-486.
16. Lash L.H. Mitochondrial glutathione in diabetic nephropathy. *J Clin Med.* **2015**, *4*, 1428-1447.
17. Aguilar M.G.; Baines C.P.; Physiological and pathological roles of mitochondrial SLC25 carriers. *Biochem J* **2013**, *454*, 371–386.
18. Coll O.; Colell A.; García-Ruiz C.; Kaplowitz N.; Fernández-Checa J.C. Sensitivity of the 2-oxoglutarate carrier to alcohol intake contributes to mitochondrial glutathione depletion. *Hepatology* **2003**, *38*, 692-702.

19. Baulies A.; Montero J.; Matías N.; Insausti N.; Terrones O.; Basañez G.; Vallejo C.; Conde de La Rosa L.; Martinez L.; Robles D.; et al. The 2-oxoglutarate carrier promotes liver cancer by sustaining mitochondrial GSH despite cholesterol loading. *Redox Biol* **2018**, *14*, 164-177.
20. Kelly-Aubert M.; Trudel S.; Fritsch J.; Nguyen-Khoa T.; Baudouin-Legros M.; Moriceau S.; Jeanson L.; Djouadi F.; Matar C.; Conti M.; Ollero M.; Brouillard F.; Edelman A. GSH monoethyl ester rescues mitochondrial defects in cystic fibrosis models. *Hum Mol Genet* **2011**, *20*, 2745-2759.
21. Chung B.Y.; Choi S.R.; Moon I.J.; Park C.W.; Kim Y.H.; Chang S.E. The Glutathione Derivative, GSH Monoethyl Ester, May Effectively Whiten Skin but GSH Does Not. *Int J Mol Sci* **2016**, *17*, pii: E629.
22. Chen T.; Turner B.J.; Beart P.M.; Sheehan-Hennessy L.; Elekwachi C.; Muyderman H. Glutathione monoethyl ester prevents TDP-43 pathology in motor neuronal NSC-34 cells. *Neurochem Int* **2018**, *112*, 278-287.
23. Aminizadeh N.; Tiraihi T.; Mesbah-Namin S.A.; Taheri T. Stimulation of cell proliferation by glutathione monoethyl ester in aged bone marrow stromal cells is associated with the assistance of TERT gene expression and telomerase activity. *In Vitro Cell Dev Biol Anim* **2016**, *52*, 772-781.
24. Jarrett S.G.; Lin H.; Godley B.F.; Boulton M.E. Mitochondrial DNA damage and its potential role in retinal degeneration. *Prog Retin Eye Res* **2008**, *27*, 596-607.
25. Hyttinen J.M.T.; Błasiak J.; Niittykoski M.; Kinnunen K.; Kauppinen A.; Salminen A.; Kaarniranta K. DNA damage response and autophagy in the degeneration of retinal pigment epithelial cells-Implications for age-related macular degeneration (AMD). *Ageing Res Rev* **2017**, *36*, 64-77.
26. Karunadharma P.P.; Nordgaard C.L.; Olsen T.W.; Ferrington D.A. Mitochondrial DNA damage as a potential mechanism for age-related macular degeneration. *Invest Ophthalmol Vis Sci* **2010**, *51*, 5470-5479.
27. Terluk M.R.; Kapphahn R.J.; Soukup L.M.; Gong H.; Gallardo C.; Montezuma S.R.; Ferrington D.A. Investigating mitochondria as a target for treating age-related macular degeneration. *J Neurosci* **2015**, *35*, 7304-7311.
28. Ferrington D.A.; Kapphahn R.J.; Leary M.M.; Atilano S.R.;Terluk M.R.; Karunadharma P.; Chen G.K.J.; Ratnapriya R.; Swaroop A.; Montezuma S.R.; Kenney M.C. Increased Retinal mtDNA Damage in the CFH Variant Associated with Age-Related Macular Degeneration. *Exp Eye Res* **2016**, *145*, 269–277.
29. Mårtensson J.; Lai J.C.; Meister A. High-affinity transport of glutathione is part of a multicomponent system essential for mitochondrial function. *Proc Natl Acad Sci USA* **1990**, *87*, 7185-7189.
30. Sreekumar P.G.; Hinton D.R.; Kannan R. Glutathione Metabolism and its contribution to antiapoptotic properties of alpha crystallins in the retina. In *Oxidative Stress in Applied Basic Research and Clinical Practice;* Stratton R.D., Hauswirth W.W., Gardner T.W.; Eds; Springer Medical Publishing Company: Springer New York, USA, 2012, pp. 181-202.
31. Palmieri F. The mitochondrial transporter family SLC25: identification, properties and physiopathology. *Mol Aspects Med* **2013**, *34*, 465-84.
32. Chen Z; Lash L.H. Evidence for mitochondrial uptake of glutathione by dicarboxylate and 2-oxoglutarate carriers. *J Pharmacol Exp Ther* **1998**, *285*, 608-618.
33. Chen Z.; Putt D.A.; Lash L.H. Enrichment and functional reconstitution of glutathione transport activity from rabbit kidney mitochondria: further evidence for the role of the dicarboxylate and 2-oxoglutarate cirriers in mitochondrial glutathione transport. *Arch Biochem Biophys.* **2000**, *373*,193–202.
34. Booty L.M.; King M.S.; Thangaratnarajah C.; Majd H.; James A.M., Kunji E.R.; Murphy M.P. The mitochondrial dicarboxylate and 2-oxoglutarate carriers do not transport glutathione. *FEBS Lett* **2015**, *589*, 621-628.
35. Wilkins H.M.; Brock S.; Gray J.J.; Linseman D.A. Stable over-expression of the 2- oxoglutarate carrier enhances neuronal cell resistance to oxidative stress via Bcl-2-dependent mitochondrial GSH transport. *J. Neurochem* **2014**, *130*, 75–86.
36. Zheng L.; Cardaci S.; Jerby L.; MacKenzie E.D.; Sciacovelli M.; Johnson T.I. Fumarate induces redox-dependent senescence by modifying glutathione metabolism. *Nat Commun* **2015**, *6*, 6001.
37. Zhu D.; Deng X.; Spee C.; Sonoda S.; Hsieh CL.; Barron E.; Pera M.; Hinton DR. Polarized secretion of PEDF from human embryonic stem cell-derived RPE promotes retinal progenitor cell survival. *Invest Ophthalmol Vis Sci* **2011**, *52*, 1573-1585.
38. Sonoda S.; Sreekumar P.G.; Kase S.; Spee C.; Ryan S.J.; Kannan R., Hinton D.R. Attainment of polarity promotes growth factor secretion by retinal pigment epithelial cells: relevance to age-related macular degeneration. *Aging* **2009**, 2, 28-42.

39. Wang W.; Sreekumar P.G.; Valluripalli V.; Shi P.; Wang J.; Lin Y.A.; Cui H.; Kannan R.; Hinton D.R.; MacKay J.A. Protein polymer nanoparticles engineered as chaperones protect against apoptosis in human retinal pigment epithelial cells. *J Control Release* **2014**, *191*, 4-14.
40. Sonoda S.; Spee C.; Barron E.; Ryan S.J.; Kannan R.; Hinton D.R. A protocol for the culture and differentiation of highly polarized human retinal pigment epithelial cells. *Nature Protocols* **2009**, *4*, 662-673.
41. Sreekumar P.G.; Li Z.; Wang W.; Spee C.; Hinton D.R.; Kannan R.; MacKay J.A. Intra-vitreal αB crystallin fused to elastin-like polypeptide provides neuroprotection in a mouse model of age-related macular degeneration. *J Control Release* **2018**, *283*, 94-104.